Chapter 5

Geochronology

5.1 Introduction

The Cenozoic strata of the Kalahari Formation can be subdivided into two distinct parts. The lower part is composed of lacustrine, fluvial and terrestrial sediments of Paleocene (ca. 60 Ma) to Pliocene age that cover large parts of the interior of southern Africa (Partridge and Maud, 1987). Increasingly arid climatic conditions resulted in extensive calcretization of these sediments (King, 1962, Netterberg, 1969b, Watts, 1980), a process that may have commenced in the Middle Pliocene (Burke, 1996) and is still ongoing. A thin veneer of windblown Kalahari sands then covered the calcretized sediments during Peistocene and recent times. These so-called Hutton sands constitute the upper part of the Kalahari Formation.

The relative and absolute timing of the events that constitute this conceptual regional geological framework have remained the subject of controversial debate due to the lack of accurate age constraints. The depositional age of the sediments of the lower part of the Kalahari Formation and the age of calcretization are only very poorly constrained. Consequently, the age and duration of supergene alteration of manganese ores of the Kalahari manganese field along the Kalahari unconformity remain uncertain. Fortunately the presence of potassium in supergene ores below the Kalahari unconformity make $^{40}Ar/^{39}Ar$ dating of the formation of supergene ores possible.

Recent studies (Vasconcelos et al., 1992; Vasconcelos et al., 1994; Dammer et al. , 1996; Ruffet et al., 1996; Vasconcelos, 1999 Hautmann and Lippolt, 2000) have illustrated that K-bearing Mn^{4+} oxyhydroxides, especially those of the manganomelane group, are well suited for $^{40}Ar/^{39}Ar$ dating. Dating of this group of minerals in soils and weathering profiles has been successfully applied to unravel the age and duration of weathering processes and to match the results with patterns of paleoclimatic change (Vasconcelos, 1999). Todorokite, with a larger tunnel structure than manganomelane, contains only

small concentrations of potassium (Gutzmer and Beukes, 2000) and its suitability for $^{40}Ar/^{39}Ar$ dating is uncertain (Vasconcelos, 1999). It is the purpose of this contribution to document the results of an attempt to date todorokite- and manganomelane-rich supergene ores from the Rissik area by the laser-heating $^{40}Ar/^{39}Ar$ method.

5.2 Methods

For the purpose of this study a drill core intersection was sampled through the strongly supergene altered central and lower portions of the lowermost manganese orebody of the Hotazel Formation along the eastern suboutcrop perimeter of the main Kalahari deposit. The studied drill core Rex2 (Fig. 5.1) from the farm Rissik was selected, because the Kalahari unconformity rests directly on lithostratigraphic zones M, C and N (Nel et al., 1986) that constitute the economically important central part of the lower manganese ore bed (Nel et al., 1986) with well-established mineralogical and geochemical characteristics (Nel et al., 1986; Kleyenstüber, 1984; Preston, 2001).

The drill core intersection of the lower manganese ore bed in drill core Rex 2 was quartered along its entire length. One of the quarters was sampled for this study. This quarter was then again split into two portions along its entire length, with one half retained for the preparation of polished thin sections and $^{40}Ar/^{39}Ar$ dating and the other half were used for geochemical analysis done by Mintek.

Drill core samples were visually investigated, and the most indurated manganese oxide horizons were selected for analysis. The samples were crushed using a pair of pliers and five 1-2 mm grains from selected indurated horizons were hand-picked. The grains were ultrasonically cleaned for 30-60 minutes in distilled water, and again in absolute ethanol.$^{40}Ar/^{39}Ar$ geochronology studies for the M,C N, and B-zones were conducted at UQ-AGES (University of Queensland Argon Geochronology in Earth Sciences laboratory), Brisbane, Australia. Mn-ore grains were loaded into aluminum irradiation disks together with Fish Canyon sanidine neutron flux monitors according to the

geometry illustrated in Vasconcelos et al. (2002). The disks were irradiated for 14 hours at the CLICIT facility in the Oregon State University Radiation Center Triga Reactor. After a 6-week cooling period, the standards were analyzed by the laser total fusion method, yielding J factors of 0.003702 ± 0.00000355 and 0.003688 ± 0.00000302 for the two discs containing the manganese oxide samples (J factor for each sample shown in Table 2). Other irradiation correction factors are: (2.64 ± 0.02) x 10^{-4} for $(^{36}Ar/^{37}Ar)_{Ca}$, (7.04 ± 0.06) x 10^{-4} for $(^{39}Ar/^{37}Ar)_{Ca}$ and (8 ± 3) x 10^{-4} for $(^{40}Ar/^{36}Ar)_{K}$. Twenty seven manganese oxide grains, extracted from 9 distinct samples, were analyzed by the laser incremental heating method (a minimum of 9 and a maximum of 18 steps per grain) following the procedure described in Vasconcelos (1999a) and Vasconcelos et al. (2002). Air pipettes and full system blanks were analyzed before and after each grain, yielding $^{40}Ar/^{36}Ar$ discrimination values ranging from 1.0045 ± 0.0018 to 1.0075 ± 0.0018. All dates are reported using 5.543 x 10^{-10} a^{-1} as the total decay constant for ^{40}K (Steiger and Jäger, 1978).

Only the M, C and N-zones produced useful $^{40}Ar/^{39}Ar$ step heating results. Results obtained for samples from the B-zone were in general very complex and variable, possibly because the B-zone contains anomalous high Fe-concentrations, which appear to prevent accurate age dating for an as yet unknown reason (Vasconcelos, 1999).

5.3 Mineralogy and Petrography of Sampled Intervals

X-ray powder diffraction and microscopic studies were used to semi-quantitatively determine the mineralogical composition of all 5 lithostratigraphic zones of the lower manganese orebody intersected in drill core Rex 2 (Fig. 5.1). The fine-grained carbonate-rich mineral assemblage (Nel et al., 1986) characteristic of the carbonate-rich braunite lutite protore is extensively altered in all five manganiferous zones of the lower ore body intersected in drill core Rex 2. Supergene alteration is mostly on the expense of protore Mn-carbonates, with minor kutnahorite preserved only in zone C. Other carbonates (M, C, N zones: kutnahorite, Mn-calcite; B, L zones: rhodochrosite; Kleyenstüber, 1985) are notably absent. The occurrence of calcite in zone M, immediately below the Kalahari unconformity, is attributed to the presence of microscopic calcrete-filled fractures. Oxide

minerals of the protore assemblage (M, C, N zones: braunite, hausmannite, hematite; B zone: jacobsite, hematite; L zone: hematite; Nel et al., 1986) appear much less affected by supergene alteration than carbonates (Fig. 5.2).

Supergene oxidation products of the protore assemblage include todorokite, manganomelane, minor pyrolusite and quartz (Table 5.1). These minerals are typically microcrystalline (grain sizes generally below 1 µm) and very intimately intergrown with residual protore mineral grains (Fig. 5.2a). The submicroscopic intergrowth causes obvious problems to obtain reliable analyses of any of the matrix minerals even by microprobe techniques. The finely intergrown todorokite and manganomelane present in the crosscutting veinlets are more indurated than the todorokite-rich material that constitutes the matrix.

Table 5.1. Mineralogical composition for each lithostratigraphic zone in drill core Rex 2. Abbreviations: Brnte = Braunite, Hem = Hematite, Todo = Todorokite, Jacob = Jacobsite, Man = Manganomelane, Pyr = Pyrolusite xxxx = Dominant phase (> 50%), xxx = Major phase (20 – 50%), xx = Minor phase (5 – 20%), x = Trace phase (< 5%).

Zone	Diagenetic mineral assemblage			Supergene mineral assemblage			Whole rock analyses (wt%)						
	Oxides			Oxides									
	Brnte	Hem	Jacob	Man	Todo	Pyr	Mn_3O_4	Fe_2O_3	MgO	CaO	K_2O	Na_2O	Ba
M	x	xx		xxx	xxx		58.8	8.26	1.98	1.91	1.22	0.53	0.84
C	xx	xx		xxxx	xxx	xx	59.8	6.73	1.96	1.38	1.23	0.38	0.74
N	x	xx		xx	xxx	xx	54.7	9.36	1.83	1.81	0.79	0.45	0.10
B		xx	xxx		xxx	xx	40.7	21.3	1.14	1.16	0.58	0.37	0.10
L		xxxx	xx		xx		29.8	30.8	0.97	0.72	0.31	0.34	0.06

Hausmannite occurs in M, C and N - Zones (x). Calcite occurs in M -Zone (xx). Serpentine occurs in M (xx) and N -Zones (xxx). Magnetite occurs in L -Zone (xxx) and quartz was observed in the B (x) and L -Zones (xx). The term Manganomelane is used to name a whole group of poorly crystalline manganese oxides as suggested by Frenzel (1980). This group includes the end members romanèchite (Ba and H_2O-rich), cryptomelane (K-rich) and manjiroite (Na-rich).

Former carbonate and hausmannite ovoids and laminae (Nel et al., 1986) in the protore assemblage are altered to porous todorokite-manganomelane aggregates, often with a zoned appearance (Fig. 5.2b). Microcrystalline matrix and ovoids are both crosscut by fracture-hosted veinlets (Fig. 5.2c) filled by compact masses of fibrous todorokite, manganomelane and microcrystalline quartz. Qualitative SEM-EDS analyses indicate that manganomelane in these veinlets is enriched in Ba (resembling romanechite in composition) in zone M, closest to the Kalahari unconformity, but becomes more K and Na-dominated with increasing distance from the suboutcrop. Supergene alteration is closely associated with a distinct porosity increase. The carbonate-rich protore is very

dense and virtually devoid of porosity, while porosities of strongly supergene altered manganese ore range from 10-30 vol% (Figs. 5.2a and b).

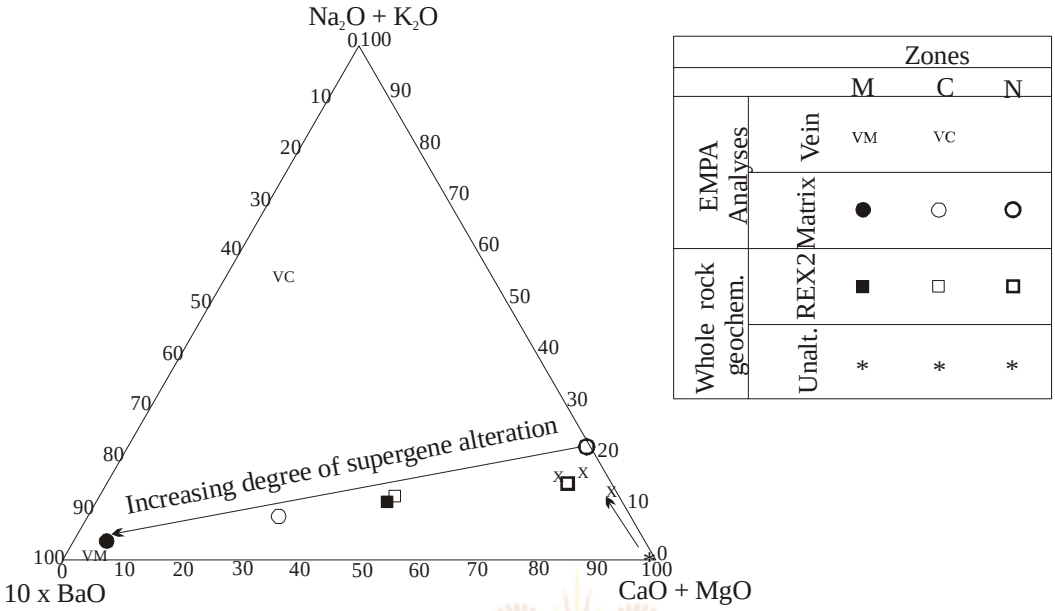

Figure 5.3. Ternary plot of Na_2O+K_2O, CaO+MgO and BaO contents of the matrix, cross-cutting veinlets and whole rock composition of Rex 2 and an unaltered sample (Unalt.) of the lithostratigraphic M, C and N-Zones. The composition of todorokite in Rex 2 is compared to the composition of todorokite reported by Gutzmer and Beukes (2000) (indicated by x).

The observed mineralogical transformations are in good agreement with whole rock geochemistry and careful microprobe analyses of microscrystalline Mn-oxihydroxides in the supergene altered matrix in zones M, C, and N (Fig. 5.3). The ternary diagram of (CaO+MgO) – (Na_2O+K_2O) – (10xBaO) (all in molar abundances) documents the relative abundance of romanechite (Ba-rich manganomelane), manjiroite/cryptomelane (Na_2O-, K_2O-rich manganomelane) and carbonate/todorokite (CaO+MgO) (Fig. 5.3). Samples of unaltered braunite lutite from a reference dill core (REX-U), also from the southernmost portion of the Kalahari deposit, plot consistently into the (CaO+MgO) corner suggesting that alkali elements and Ba are introduced into the manganese ore by meteoric water during supergene alteration. An increasing degree of supergene alteration towards the Kalahari Unconformity, as documented by the lithostratigraphic zones N, C and M (Fig. 5.1) results first in an abrupt increase of Na and K – on the expense of Ca

and Mg, followed by a gradual increase of BaO at constant $(Na_2O+K_2O)/(CaO+MgO)$ ratio (Fig. 5.3). The latter trend is in excellent agreement with the observation of an abundance of romanechite veinlets especially in the M zone, immediately below the Kalahari Unconformity.

5.4 $^{40}Ar/^{39}Ar$ Analyses

Analytical results and calculated apparent ages for each step in the 27 grains analyzed by the incremental heating method are summarized in Appendix 5. Incremental heating spectra for each grain analyzed are shown in Fig's. 5.4 and 5.5. The spectra illustrate the complexity of the system. Some grains yield well-defined plateaus (e.g., 2028-03, 2050-01 (Fig. 7)), where more than 50% of the ^{39}Ar is released in 2 or more contiguous steps within error from the mean. However, several grains yield ascending (e.g., 2048-01 (Fig. 5.4M)) spectra, other grains show clear evidence of ^{39}Ar recoil (e.g., 2028-02 (Fig. 5.5K)), while some grains show the presence of contaminants (e.g., 2026-02 (Fig. 5.4B)) (Vasconcelos, 1999). Another troubling result is the fact that some samples analyzed in triplicate may show a large range of results among the three grains ((e.g., 2047-01,-02, and -03) (Fig's. 5.4J, K and L)). Several geological and analytical factors may explain the complexity of the results (mixed-age populations; composite grains containing several different minerals; composite grains containing several different generations of a mineral; contamination of the supergene phase by unweathered or partially weathered hypogene mineral; ^{39}Ar recoil; ^{40}Ar loss during the geological history of the sample or during sample preparation; etc.) (Vasconcelos et al., 1994). To avoid some of the uncertainties above, it is always useful to perform mineralogical analysis (scanning electron microscopy, electron microprobe analysis, x-ray diffractometry, etc.) on grains extracted from the same population selected for $^{40}Ar/^{39}Ar$ geochronology. However, this approach was not feasible in this study due to the extremely fine-grained nature of the material.

Nevertheless, the mineralogical work performed on the same drill core clearly show that a single 1-2 mm grain may contain several mineral phases (Table 5.1). In addition, the mineralogical work also shows abundance of todorokite, a phase that Vaconcelos (1999b)

suggested as poorly suitable for $^{40}Ar/^{39}Ar$ geochronology. However, during sample preparation for $^{40}Ar/^{39}Ar$ geochronology we carefully selected the more indurated bands in the drill cores, which previous experience indicates are composed of finely intergrown manganomelane and todorokite, as opposed to the soft, more open todorokite-rich ores.

For the reasons stated above, the complexities of some of the spectra are interpreted as indicating the presence of several generations of intimately intergrown supergene manganese oxyhydroxides. The fine-grained nature of the minerals analyzed also explains the large uncertainty in some of the results as a consequence of the large amount of atmospheric argon trapped in intercrystalline space (Vasconcelos et al., 1995).

Despite these reservations above, two observations are very encouraging: (1) the fact that, for the majority of the samples, the three grains analysed yield similar spectra and results; and (2) the fact that the data yield a trend from older results close to the surface to younger results toward the bottom of the profile, as would be expected in a typical weathering profile (Vasconcelos, 1999a). To illustrate this age progradation from the surface toward the bottom of the profile, we plotted a probability-density plot (Fig. 5.6) for the complete data set, grouping the samples according to their source zone (Fig. 5.1). The most probable ages (highest probability peak for each generation) range from 26.76 for the uppermost M-Zone, to 10.06 Ma to the intermediate C-Zone, and 5.23 Ma to the lowermost N-Zone. This trend is also identified by the weighted mean averages of the all the results for each zone, which ranges from 31 ± 5, 20 ± 2, and 4.3 ± 1 Ma for the M-, C- and N-zones, respectively.

The broad shape of the probability density plot, and the increase in the probability peak towards younger results suggest that mixed generations of supergene phases likely occur in all samples analyzed. The older, near surface samples, are exposed to the weathering solutions responsible for the formation of the younger generations at the bottom of the profile, and are partially recrystallized during the more recent weathering events, decreasing the precision of the ages obtainable for the older generations.

5.5 Summary

The Ar-Ar dating of microcrystalline todorokite-manganomelane mixtures developed along the Cenozoic Kalahari unconformity in the Kalahari manganese field yields results characteristic for other weathering profiles as reported by Vasconcelos (1999). The distribution of apparent ages, as illustrated by the probability plot (Fig. 5.6) becomes less complex towards younger ages. In turn, these younger $^{40}Ar/^{39}Ar$ ages are observed down in the section, with increasing distance below the pre-Kalahari erosional unconformity. This results in an apparent inversion of the stratigraphy, explained by the downward progression of the weathering front into the Mn-ore body through time (Vasconcelos et al., 1994). Compared to manganese-rich lateritic caps developed on Mn-carbonate deposits in South America (Vasconcelos, 1999), West Africa (Vasconcelos, 1999; Vasconcelos et al., 1994) and Australia (Vasconcelos, 1999), results from the Kalahari manganese field are rather complex, with few grains yielding well-developed plateau or integrated ages. Reasons for the apparent complexity may be the extreme fine-grained nature of the supergene mineral assemblage, its intimate intergrowth with residues of the precursor braunite-lutite assemblage, and the predominance of todorokite, a mineral regarded by Vasconcelos (1999) as poorly suited for ^{40}Ar-^{39}Ar dating. Despite these complications there are some very interesting conclusions that can be derived from the available data set. Oldest apparent age steps that are at about 43 Ma in the M-zone immediately below the Kalahari Unconformity are in very good agreement with ages reported in Gutzmer and Beukes (2000) for asbestiform manjiroite-todorokite veins developed in the Smartt-Rissik area (36.3 and 42.6 Ma). Finally, the probability plot obtained for the lowermost N-zone is marked by a very well defined peak at ca. 5 Ma which most probably documents the last phase of supergene alteration in the Kalahari manganese field below the Kalahari Formation.